Configurational entropy of adsorbed particles on two-dimensional heterogeneous surfaces

F. Romá, A.J. Ramirez-Pastor*

Departamento de Física, Universidad Nacional de San Luis, CONICET Chacabuco 917, San Luis 5700, Argentina

Abstract

The configurational entropy of repulsive interacting particles adsorbed on heterogeneous surfaces is studied by combining Monte Carlo simulation and thermodynamic integration method. The substrate is represented by a bivariate lattice characterized by $l \times l$ patches of weak and strong adsorbing sites, arranged in a deterministic chessboard structure. The temperature is varied in such a way that different ordered phases can be formed on the surface. A rich variety of behaviors is found and analyzed in the context of the lattice-gas model.
© 2003 Elsevier B.V. All rights reserved.

1. Introduction

The advantages of using Monte Carlo simulation to calculate thermal averages of thermodynamic observables are well known [1]. The estimation of certain quantities such as total energy, energy fluctuations, correlation functions, etc., is rather straightforward from averaging over a large enough number of instantaneous configurations (states) of a thermodynamic system. However, free energy and entropy, in general, cannot be directly computed. In order to calculate free energy and entropy, various methods have been developed. Namely, thermodynamic integration method

---

* Corresponding author. Tel.: +54-2652-436151; Fax: +54-2652-430224.
  E-mail address: antorami@unsl.edu.ar (A.J. Ramirez-Pastor).

(TIM) [2–7], Ma's method of coincidence counting of states along the trajectory in phase space [8], "stochastic models"—method of Alexandrowicz [9], "local states"—method of Meirovitch [10], "multistage sampling" and "umbrella sampling" of Valleau et al. [11,12], method of Salsburg [13], method of Yip et al. [14] (which is an optimized combination of coupling parameter and adiabatic switching formalisms), etc. Among them, the TIM is one of the most widely used and practically applicable. The method relies upon integration of the total energy on temperature along a reversible path between an arbitrary reference state and the desired state of the system.

On the other hand, theoretical studies have been devoted to the configurational entropy of adsorbed monoatomic and polyatomic molecules. In this sense, by using the transfer matrix method, Phares et al. [15–19] studied the configurational entropy of interacting particles (dimers and monomers) adsorbed on lattices with different geometries. In these leading contributions, a rich variety of different behaviors and structural orderings were found and discussed by the authors.

In all previously mentioned cases, the surface is considered to be chemically homogeneous and smooth. However, real surfaces generally present inhomogeneities due to irregular arrangement of surface and bulk atoms or the presence of various chemical species, which can significantly affect the main thermodynamics functions. Therefore, increasing interest and efforts have been devoted over decades to developing a deeper understanding of the surface heterogeneity [20–23]. Most of the papers dealing with molecular processes on heterogeneous surfaces have been dedicated to the analysis of phenomena such as diffusion [24], percolation [25], growth [26], adsorption isotherms and heats of adsorption [27], multisite occupancy [28], etc. As it was discussed above, the entropy is much more difficult to evaluate and, in the best knowledge of the authors, there is still a lack of systematic studies on the behavior of the adsorbate's entropy in presence of surface heterogeneity. For these reason, it is of interest and of value to inquire how a specific lattice structure (heterogeneous surface with intermediate correlation) influences the entropy of the adlayer.

In this context, the main objective of our paper is to determine, via Monte Carlo simulation and thermodynamic integration method in canonical ensemble, the effects of the surface heterogeneity on the behavior of the configurational entropy of adsorbed interacting particles. For this purpose, we consider a gas of monomers adsorbed on bivariate heterogeneous surfaces with a characteristic correlation length, l. The bivariate surfaces are composed by two kinds of sites, say weak and strong sites with adsorptive energies ε_1 and ε_2, respectively, arranged in patches of size l with a chessboard structure. A special class of this kind of surface has been observed recently to occur in a natural system [29], although it was already intensively used in modeling adsorption and surface diffusion phenomena [24–28].

The plan of the rest of paper is as follow. In Section 2 the lattice-gas model is given along with the basis of the thermodynamic integration method in canonical ensemble. The results are presented in Section 3. Finally, we close this article in Section 4 with the conclusions.

2. Basic definitions

2.1. The model

We assume that the substrate is represented by a two-dimensional square lattice of $M = L \times L$ adsorption sites, with periodic boundary conditions. Each adsorption site can be either a "weak" site, with adsorptive energy ε_1, or a "strong" site, with adsorptive energy ε_2 ($\varepsilon_1 \leqslant 0$, $\varepsilon_2 \leqslant 0$ and $|\varepsilon_1| < |\varepsilon_2|$). Weak and strong sites form square patches of size $l(l = 1, 2, 3, \ldots)$ which are spatially distributed in a deterministic alternate way (chessboard topography), Fig. 1.

In order to describe the system of N particles adsorbed on M sites at a given temperature T, let us introduce the occupation variable c_i, which can take the values $c_i = 0$ if the corresponding site is empty and $c_i = 1$ if the site is occupied. Particles can be adsorbed on the substrate with the restriction of at most one adsorbed particle per site and we consider a nearest neighbor (NN) repulsive interaction energy w among them. Under these considerations, the Hamiltonian of the system is given by

$$H = w \sum_{(i,j)'} c_i c_j + \sum_i^M \varepsilon_i c_i , \tag{1}$$

where $(i, j)'$ represents pairs of NN sites and $\varepsilon_i (= \varepsilon_1$ or $\varepsilon_2)$ is the energy of adsorption of one given surface site.
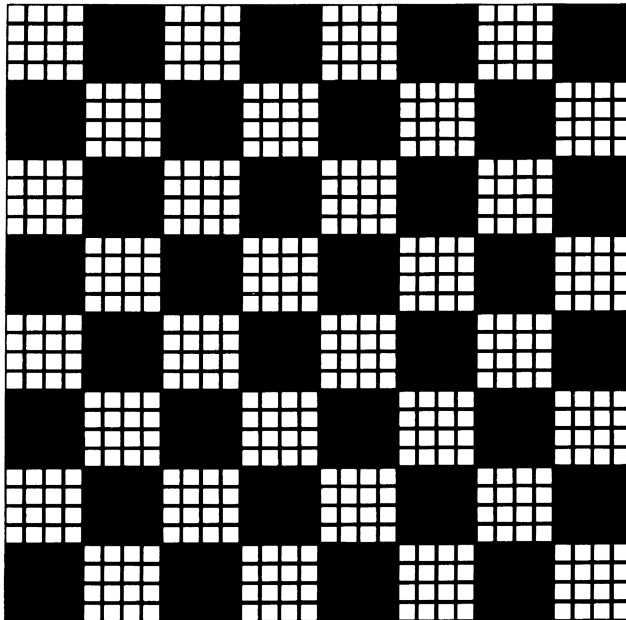

Fig. 1. Schematic representation of a square heterogeneous bivariate surface with chessboard topography. Black (white) symbols represent sites with energy ε_1 (ε_2). The patch size in this figure is $l = 4$.

2.2. Thermodynamic integration method in canonical ensemble

Let us suppose a lattice-gas of N interacting particles, each of which occupies one site on a regular lattice with M sites at temperature T. Then, it is possible to write

$$\left(\frac{\partial S}{\partial T}\right)_{N,M} = \frac{1}{T}\left(\frac{\partial U}{\partial T}\right)_{N,M}, \tag{2}$$

where S and U represent the configurational entropy and the internal energy, respectively. From Eq. (2),

$$S(N,M,T) = S(N,M,T_o) + \int_{T_o}^{T} \frac{\mathrm{d}U}{T}. \tag{3}$$

Eq. (3) allows to calculate the entropy in different equilibrium states if $S(N,M,T_o)$ (reference state) is known, given that the integral in the second term can be accurately estimated by Monte Carlo simulation. This procedure is called thermodynamic integration.

In our case, the determination of the entropy in the reference state is trivial. In fact, for a monoatomic lattice-gas

$$\lim_{T_o \to \infty} S(N,M,T_o) = k_B \ln \binom{M}{N} = k_B \ln\left[\frac{M!}{N!(M-N)!}\right]. \tag{4}$$

k_B being the Boltzmann constant. By using the Stirling's approximation ($\ln x! \approx x \ln x - x$), Eq. (4) can be written as $s(\theta, T_o \to \infty)/k_B = -\theta \ln \theta - (1-\theta)\ln(1-\theta)$, where $\theta = N/M$ and $s = S/M$ denote surface coverage and entropy per site, respectively.

On the other hand, the integral in the second term of Eq. (3) can be obtained by evaluating U at constant coverage for various values of T following the standard procedure of Monte Carlo simulation in the canonical ensemble, based on the Metropolis scheme [30]. Then, $U(T)$ is spline-fitted and numerically integrated [5–7].

The approximation to thermodynamical equilibrium is usually reached in 10^6 MCS (a Monte Carlo Step (MCS) is achieved when M sites have been tested to change its occupancy state). After that, mean values of the internal energy U, are obtained by simple averages over 10^6 MCS configurations. In the next section, we analyze the application of this methodology in calculating adsorption entropy of interacting particles adsorbed on two-dimensional heterogeneous surfaces.

3. Results

The computational simulations have been developed for squares $L \times L$ lattices with $L = 144$ (in such a way that it is a multiple of l) and periodic boundary conditions. With this size of the lattice we verified that finite size effects, which affect the thermodynamical properties in the case of repulsive interactions at much smaller sizes, are negligible. We focus on the case of repulsive interaction energy among adsorbed particles ($w > 0$). This is far more interesting since, as we shall see, order–disorder transitions can take place in the adsorbate, even if the order can be partially disturbed by heterogeneity.
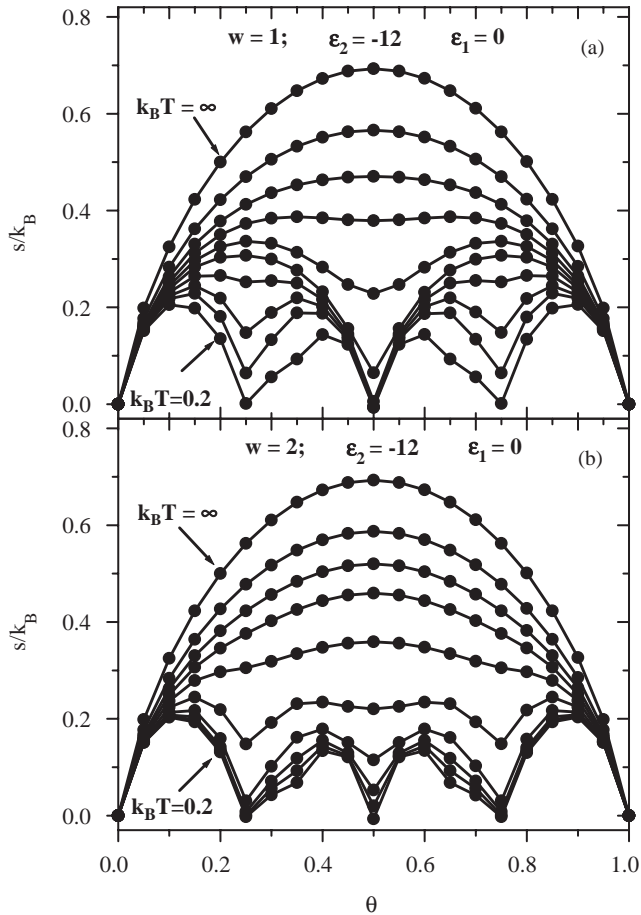
Fig. 2. Configurational entropy per site (in units of k_B) versus the surface coverage for interacting particles adsorbed in chessboard substrates with $l = 12$ and $\Delta\varepsilon = 12$. The curves from top to bottom correspond to the following: $k_BT = \infty$, $k_BT = 4.90$, $k_BT = 3.30$, $k_BT = 2.50$, $k_BT = 1.67$, $k_BT = 1.00$, $k_BT = 0.67$, $k_BT = 0.50$, $k_BT = 0.40$ and $k_BT = 0.2$, respectively. (a) $w = 1$, (b) $w = 2$.

The difference between the energies of the patches has been chosen to be $\Delta\varepsilon = \varepsilon_1 - \varepsilon_2 = 12$ ($\varepsilon_1 = 0, \varepsilon_2 = -12$). A high value of $\Delta\varepsilon$ has been considered in order to emphasize the effect of the surface heterogeneity as the temperature is diminished.

In order to understand the basic phenomenology, we consider in first place a chessboard topography with $l = 12$ (size of each homogeneous patch), and different values of the temperature. Fig. 2(a) [(b)] shows canonical Monte Carlo simulations of the configurational entropy per site, s, versus surface coverage, θ, for $w = 1$ [$w = 2$]. As a consequence of the equivalence particle-vacancy, the curves are symmetrical around $\theta = 0.5$. For high temperatures, the overall behavior can be summarized as follows: in the limits $\theta \to 0$ and $\theta \to 1$ the entropy tends to zero. For very low coverages

$s(\theta)/k_B$ is an increasing function of θ, reaches a maximum at $\theta = 0.5$, then decreases monotonically to zero for $\theta > 0.5$.

As the temperature is diminished, the entropy decreases for all coverage and develops three local minima at $\theta = \frac{1}{4}$, $\frac{1}{2}$ and $\frac{3}{4}$. In the ground state, $s\left(\theta = \frac{1}{4}, T = 0\right)/k_B = s\left(\theta = \frac{1}{2}, T = 0\right)/k_B = s\left(\theta = \frac{3}{4}, T = 0\right)/k_B = 0$. These marked singularities are separating four different adsorption processes: (i) for $0 < \theta < \frac{1}{4}$, the strong site patches are filled until the $c(2 \times 2)$ ordered phase is formed on them; (ii) for $\frac{1}{4} < \theta < \frac{1}{2}$, the filling of the strong site patches is completed; (iii) for $\frac{1}{2} < \theta < \frac{3}{4}$, the weak site patches are filled until the $c(2 \times 2)$ ordered phase is formed on them; (iv) for $\frac{3}{4} < \theta < 1$, the filling of the weak site patches is completed.

We now analyze the case corresponding to $w = 4$ (Fig. 3(a)) and $w = 5$ (Fig. 3(b)). As in Fig. 2, three minima appear in the entropy as T decreases. Nevertheless, the cause of these minima in Figs. 3(a) and (b) is different. In fact, the filling of the lattice proceeds according to the following processes: (i) for $0 < \theta < \frac{1}{4}$, the strong site patches are filled until the $c(2 \times 2)$ ordered phase is formed on them; (ii) for $\frac{1}{4} < \theta < \frac{1}{2}$, the weak site patches are filled until the $c(2 \times 2)$ ordered phase is formed on them; (iii) for $\frac{1}{2} < \theta < \frac{3}{4}$, the filling of the strong site patches is completed; (iv) for $\frac{3}{4} < \theta < 1$, the filling of the weak site patches is completed.

As it can be easily understood, once strong site patches are filled up to $\theta = 0.25$ (where a $c(2 \times 2)$ structure is formed on them), there are two possible positions to adsorb a new particle: (1) on strong sites, involving an energy of $4w + \varepsilon_2$ ($4w$ due to repulsions); or (2) on weak sites, with energy ε_1. Then, as long as the condition $4w + \varepsilon_2 < \varepsilon_1$ $\left(w/\Delta\varepsilon < \frac{1}{4}\right)$ is satisfied, the adsorption process is similar to the one described in Fig. 2, i.e. strong site patches are filled first and weak site patches are filled after. We call this feature regime I (RI).

On the other hand, the condition $\varepsilon_1 < 4w + \varepsilon_2$ is not suficient to assure the existence of a new regime. In fact, an intermediate adsorption regime occurs for $3w + \varepsilon_2 < \varepsilon_1 < 4w + \varepsilon_2$ $\left(\frac{1}{4} < w/\Delta\varepsilon < \frac{1}{3}\right)$, where incoming particles (at $\theta > 0.25$) can be adsorbed on the border of the strong patches (with energy $3w + \varepsilon_2$). Then, as long as $3w + \varepsilon_2 > \varepsilon_1$ $\left(w/\Delta\varepsilon > \frac{1}{3}\right)$ is satisfied, the adsorption process is as in Fig. 3, which we call regime II (RII).

RI and RII could be also interpreted in terms of spatially modulated phases [31–33] (this model was introduced some years ago to study systems with competing interactions, as the model presented here). However, we consider that such description, which is very appropriate to deal magnetic systems, is out of the scope of the present work.

In the next figure, we show RI and RII from a new perspective. For this purpose, Fig. 4(a) [(b)] presents a typical low-temperature adsorption isotherm (coverage versus chemical potential, μ) in RI [RII]. Simulations corresponding to Fig. 4 were performed in grand canonical ensemble. Both adsorption regimes can be easily visualized by following the behavior of θ_1 and θ_2 versus μ, where θ_1 (θ_2) represents the partial coverage associated to sites with energy ε_1 (ε_2).

An interesting case occurs for $w = 3$ (Fig. 5). For this lateral interaction, the adsorption process is as follows: (i) the strong site patches are filled until the $c(2 \times 2)$ ordered phase is formed on them; (ii) for $0.25 < \theta < 0.75$, the particles can be adsorbed on strong patches (with energy $\varepsilon_2 + 4w = 0$) or on weak sites (with energy $\varepsilon_1 = 0$). For
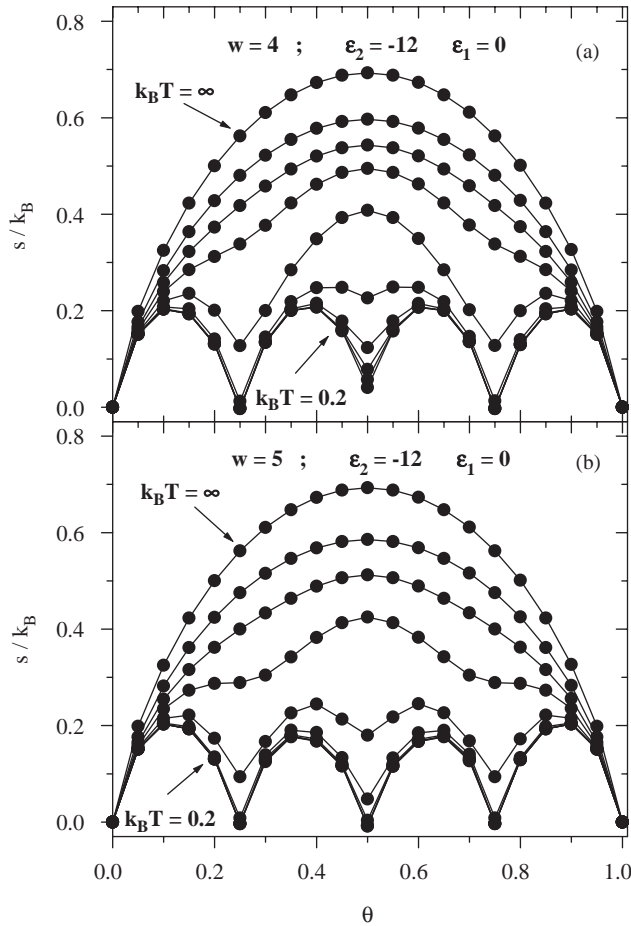
Fig. 3. Configurational entropy per site (in units of k_B) versus the surface coverage for interacting particles adsorbed in chessboard substrates with $l = 12$ and $\Delta\varepsilon = 12$. The curves from top to bottom correspond to the following: $k_B T = \infty$, $k_B T = 4.90$, $k_B T = 3.30$, $k_B T = 2.50$, $k_B T = 1.67$, $k_B T = 1.00$, $k_B T = 0.67$, $k_B T = 0.50$, $k_B T = 0.40$ and $k_B T = 0.2$, respectively. (a) $w = 4$ and (b) $w = 5$.

this reason, the entropy varies smoothly between $0.25 < \theta < 0.75$, and the minimum at $\theta = 0.5$ disappears. The process (ii) conclude when the weak site patches are filled until the $c(2 \times 2)$ ordered phase is formed on them; and finally, (iii) the filling of the weak site patches is completed.

   In the following, we will analyze what happens when the topography is changed. For this purpose, we fix the energies (lateral interaction and difference between the energies of the patches) and the temperature, and vary the size l of the patches. As in Figs. 2, 3 and 5, the Monte Carlo simulations were performed in canonical ensemble. The result of this analysis is shown in Figs. 6 and 7 for RI and RII, respectively. It can be seen that all curves vary between two limit ones: the one corresponding to
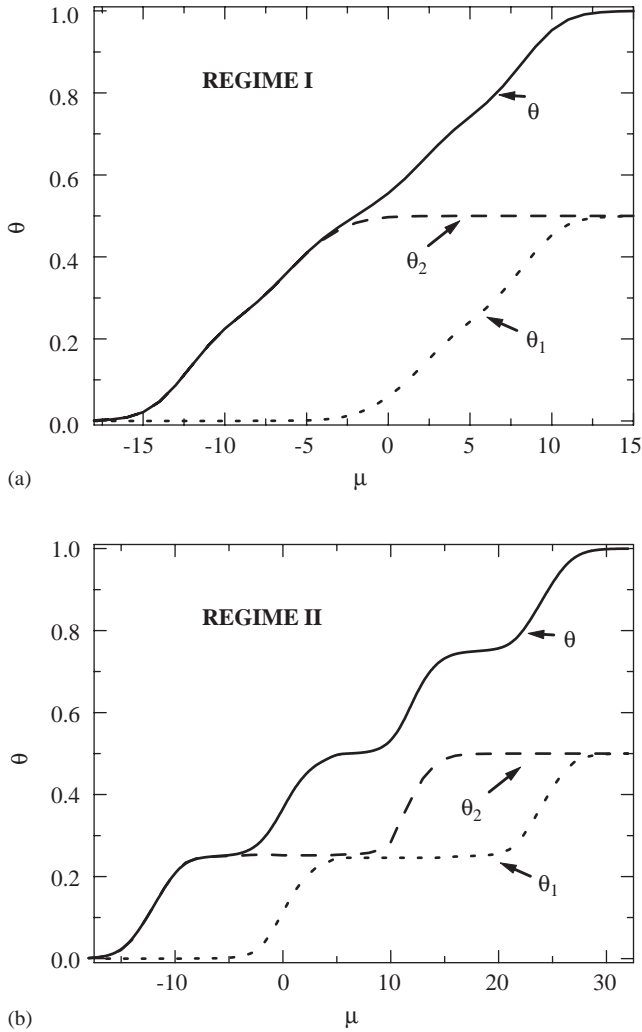
Fig. 4. Total and partials adsorption isotherms (coverage versus chemical potential μ) for a typical case in RI (a) and RII (b). Solid, dashed and dotted lines represent total coverage θ, partial coverage of strong sites θ_2 and partial coverage of weak sites θ_1, respectively.

1×1 patches and the one corresponding to bp (two big patches). The fact that the entropy for different topographies, characterized by a length scale l, vary between two extreme curves (see Figs. 6 and 7), suggests that we should search for some appropriate quantity to measure the deviation among these curves and study the behavior of such quantity as the length scale is varied. The quantity we found most suitable is

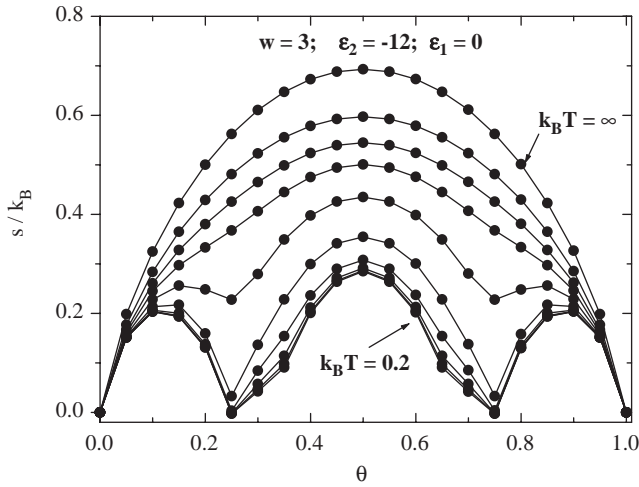$$\chi_S = \sum_i [s(\theta_i) - s^{bp}(\theta_i)]^2 , \qquad (5)$$

Fig. 5. Configurational entropy per site (in units of k_B) versus the surface coverage for interacting particles adsorbed in chessboard substrates with $l = 12$ and $\Delta\varepsilon = 12$. The curves from top to bottom correspond to the following: $k_B T = \infty$, $k_B T = 4.90$, $k_B T = 3.30$, $k_B T = 2.50$, $k_B T = 1.67$, $k_B T = 1.00$, $k_B T = 0.67$, $k_B T = 0.50$, $k_B T = 0.40$ and $k_B T = 0.2$, respectively for $w = 3$.
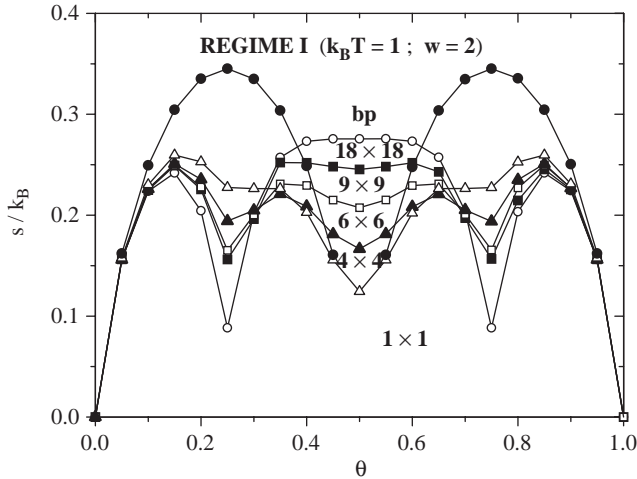

Fig. 6. Configurational entropy per site (in units of k_B) versus coverage for square chessboard topographies with different l's, $\Delta\varepsilon = 12$, $w = 2$ and $k_B T = 1$ (RI). The different values of l are displayed in the figure.

where $s^{bp}(\theta_i)$ is the entropy corresponding to big patches and the sum runs over all values of coverage (between 0 and 1). The results for χ_S are shown in Fig. 8, where we can see that χ_S behaves as a power law in l with two different values of the exponent, α_S, depending on the ratio $w/\Delta\varepsilon$. These results confirm the existence of two adsorption
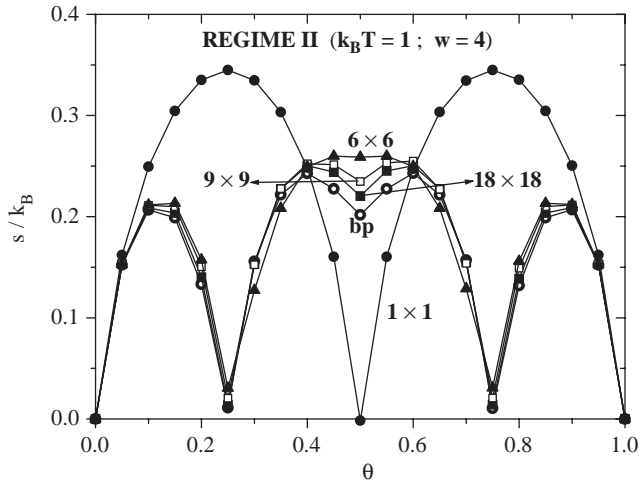
Fig. 7. Configurational entropy per site (in units of k_B) versus coverage for square chessboard topographies with different l's, $\Delta\varepsilon = 12$, $w = 4$ and $k_B T = 1$ (RII).
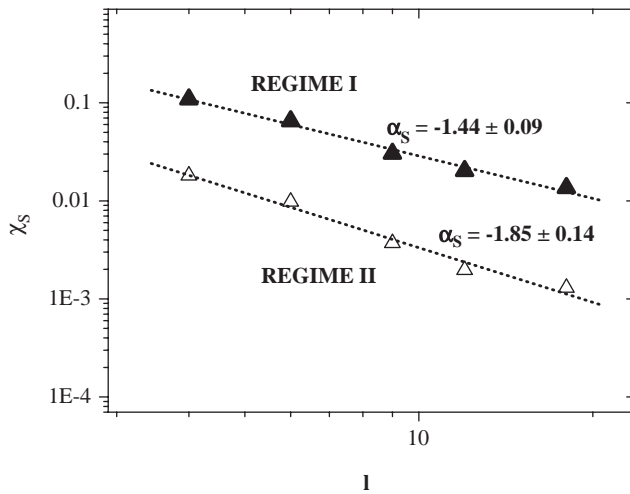

Fig. 8. Power-law behavior of the quantity χ_S showing the data for chessboard topographies in RI and RII.

regimes at low temperatures. A similar behavior was recently observed in Ref. [27] for other properties of adsorption (isotherms and differential heat of adsorption), which reinforce the robustness of the results presented here.

4. Conclusions

In the present work we have used the bivariate trap model in order to study how the surface topography affects the configurational entropy of repulsively interacting

particles. In the framework of this model, it is assumed that the surface is formed by a collection of homogeneous patches. Every adsorptive site within a given patch has the same adsorptive energy. However, different patches have different adsorptive energies. We have considered only two kinds of square patches with different energies, i.e. strong and weak patches, which are arranged in a chessboard-like ordered structure.

In order to analyze the effects of the topography on the configurational entropy of the adsorbate, three quantities have been chosen as the control parameters: (i) the relationship between the lateral interaction and the difference between the energies of the patches ($w/\Delta\varepsilon$); (ii) the temperature and (iii) the size of the patches, l, which is associated to the correlation length. On this basis, different cases have been observed:

(1) For high temperatures, the thermal energy governs the adsorption process and the entropy tends to the Langmuir case.

(2) As the temperature decreases, the configurational entropy develops three minima at coverage $\theta = 0.25$, 0.50 and 0.75, which tend to zero in the ground state ($T = 0$). Depending on the value of $w/\Delta\varepsilon$, two different regimes are observed. For $w/\Delta\varepsilon < \frac{1}{4}$ (RI), the strong sites patches are filled first and weak site patches are filled after. On the other hand, for $w/\Delta\varepsilon > \frac{1}{3}$ (RII), both patches are filled sequentially up to 50% and then, the filling of the patches is completed up to full coverage.

(3) For fixed energies and T, the configurational entropy appears as a very sensitive quantity to the correlation length, confirming the importance of the energetic correlation length as a controlling parameter in the adsorption process. This effect has been discussed in previous studies involving different process taking place on strong correlated surfaces [24–28].

Future efforts will be directed to study how (a) different topological distribution of the patches (for instance, at random); (b) different connectivities of the lattice, c ($c = 3, 4, 6$) and (c) attractive lateral interactions, influence the behavior of the entropy of interacting adsorbates on heterogeneous surfaces.

Acknowledgements

References

[1] K. Binder, Applications of the Monte Carlo Method in Statistical Physics, in: Topics in Current Physics, Vol. 36, Springer, Berlin, 1984.
[2] J.P. Hansen, L. Verlet, Phys. Rev. 184 (1969) 151.
[3] K. Binder, J. Stat. Phys. 24 (1981) 69.
[4] K. Binder, Z. Phys. B 45 (1981) 61.
[5] F. Romá, A.J. Ramirez-Pastor, J.L. Riccardo, in: D.D. Do (Ed.), Adsorption Science and Technology, World Scientific Publishing, Singapore, 2000, pp. 527–531.

[6] F. Romá, A.J. Ramirez-Pastor, J.L. Riccardo, Langmuir 16 (2000) 9406.
[7] F. Romá, A.J. Ramirez-Pastor, J.L. Riccardo, J. Chem. Phys. 114 (2001) 10 932.
[8] S.K. Ma, J. Stat. Phys. 26 (1981) 221.
[9] Z. Alexandrowicz, J. Chem. Phys. 55 (1971) 2765.
[10] H. Meirovitch, Chem. Phys. Lett. 45 (1977) 389.
[11] J.P. Valleau, D.N. Card, J. Chem. Phys. 57 (1972) 5457.
[12] G. Torrie, J.P. Valleau, Chem. Phys. Lett. 28 (1974) 578;
     G. Torrie, J.P. Valleau, J. Comput. Phys. 23 (1977) 187;
     G. Torrie, J.P. Valleau, J. Chem. Phys. 66 (1977) 1402.
[13] Z. Salsburg, J. Jacobsen, W. Fickett, W. Wood, J. Chem. Phys. 30 (1959) 65.
[14] M. de Koning, A. Antonelli, S. Yip, Phys. Rev. Lett. 83 (1999) 3973, and references therein.
[15] A.J. Phares, J. Math. Phys. 25 (1984) 1756.
[16] A.J. Phares, D.E. Shaw, F.J. Wunderlich, J. Math. Phys. 26 (1985) 1762.
[17] A.J. Phares, F.J. Wunderlich, J. Math. Phys. 26 (1985) 2491.
[18] A.J. Phares, F.J. Wunderlich, J.D. Curley, D.W. Grumbine Jr., J. Phys. A: Math. Gen. 26 (1993) 6847.
[19] A.J. Phares, F.J. Wunderlich, Phys. Rev. E 52 (1995) 2236;
     A.J. Phares, F.J. Wunderlich, Phys. Rev. E 55 (1997) 2403;
     A.J. Phares, F.J. Wunderlich, Surf. Sci. 425 (1999) 112;
     A.J. Phares, F.J. Wunderlich, Surf. Sci. 452 (2000) 108;
     A.J. Phares, F.J. Wunderlich, Surf. Sci. 479 (2001) 43.
[20] W. Rudziński, D.H. Everett, Adsorption of Gases on Heterogeneous Surfaces, Academic Press, New York, 1992.
[21] W.A. Steele, The Interaction of Gases with Solid Surfaces, Pergamon Press, New York, 1974.
[22] M.J. Jaroniec, R. Madey, Physical Adsorption on Heterogeneous Surfaces, Elsevier, Amsterdam, 1988.
[23] W. Rudziński, W.A. Steele, G. Zgrablich, Equilibria and Dynamics of Gas Adsorption on Heterogeneous Solid Surfaces, Elsevier, Amsterdam, 1996.
[24] F. Nieto, C. Uebing, V. Pereyra, R. Faccio, Surf. Sci. 423 (1999) 256.
[25] F. Nieto, A.J. Ramirez-Cuesta, R. Faccio, Phys. Rev. E 59 (1999) 3706.
[26] M. Nazzarro, F. Nieto, A.J. Ramirez-Pastor, Surf. Sci. 497 (2002) 275.
[27] F. Bulnes, A.J. Ramirez-Pastor, G. Zgrablich, J. Chem. Phys. 115 (2001) 1513;
     F. Bulnes, A.J. Ramirez-Pastor, G. Zgrablich, Phys. Rev. E 65 (2002) 31 603.
[28] J.E. González, A.J. Ramirez-Pastor, Physica A 311 (2002) 275.
[29] T.W. Fishlock, J.B. Pethica, R.G. Egdell, Surf. Sci. L 47 (2000) 445.
[30] D. Nicholson, N.D. Parsonage, Computer Simulation and the Statistical Mechanics of Adsorption, Academic Press, London, 1982.
[31] W. Selke, M.E. Fisher, Phys. Rev. B 20 (1979) 257.
[32] D.A. Huse, M.E. Fisher, J.M. Yeomans, Phys. Rev. B 23 (1981) 180.
[33] P. Upton, J.M. Yeomans, Phys. Rev. B 40 (1989) 479.